Multi-Modal AI-Driven Electrical and Optical Characterization Framework for Sub-5 nm Semiconductor Defect Localization

Srinivasa rao Gondi

Sr. Principal test engineer, NXP semiconductors San Jose, United States

Received: August 20, 2025; Revised: November 13, 2025; Accepted: December 23, 2025; Published: December 30, 2025

Abstract

This research proposes a multi-modal AI framework for characterizing electrical and optical sub-5 nm defects within a polypython–matlab co-simulation framework that electron microscopically integrates and nano electically probes optical interference. A hybrid CNN-Transformer-GNN (CTG) fusion model learns spatial and spectral relationships across heterogeneous data and topological channels. The model achieves precise defect location through contrastive feature alignment and cross-modal embedding fusion. COMSOL and TCAD simulations modeling optical near-field scattering and localized current perturbations were used to construct synthetic training datasets. Experimental evaluation shows AI multi modality models outperform single-modality models by over 40% on false positive and less than 3 nm deviation across the 3 nm and 5 nm technology node with above 3 nm localization deviation. The framework shows seamless integration with fab probes for real-time integration and self correcting inference on electron beam, scatterometry, and SEM systems. These results form an initial step towards ecosystems of augmented metrology by AI. Future work will tackle detection of defects through data-synthesis based on physics, and adaptive reinforcement data fusion EUV stochastic metrology information systems.

Keywords: Multi-Modal Metrology, Sub-5 nm Semiconductor Defects, AI Fusion Architecture, Electrical–Optical Characterization.

1 Introduction

The challenge brought by scaling semiconductor technology to the 5 nm and beyond range and its metrology and yield limiting aspects of chip manufacturing has been attributed to variability associated to the molecular and photon interaction levels. Microbridging, and the loss, merging, or breaking of contacts during EUV lithography due to random photon shot noise caused by molecular reaction kinetics and secondary electro diffusion tend to fail the micro and nano bridging commonly associated with “stochastic cliffs.” The concept that photon-resist interactions and resist blur is random and discrete and beyond control can only understood by texture and pattern formation and the associated stochastic cliffs that arise due to the variability in process control [1, 2]. The random phenomena can still be observed and the changes measured as loss of control gets exercised on parameters of device like LER and LWR which results in uncontrolled delta in threshold voltage and uncontrolled drain current in the devices which tend to be failure pathways in reliable circuits [3]. Recently, process simulations and machine learning models of virtual fabs have predicted and reduced the damaging effects caused by random processes by redistributing the parameters of resist layer and optimizing etch cycles.

Integrated metrology tools and inspection tools still provide glimpse insight into the defect landscape. SEM is still the go to tool for critical-dimension measurement and edge analysis. Atomic force microscopes have the capability of quantifying roughness and capturing high-resolution topography. Techniques such as electrical-beam induced current and electron-beam absorbed current have the ability to localize electrical

discontinuities with high precision, and optical inspection techniques—scatterometry, ellipsometry and photoluminescence—lay claim to optical defect detection of a surface and the subsurface. Still, no single technique describes the defect physics. Detection of stochastic defects using SEM is a valuable technique, but it has has a significant sensitivity deficiency and high rate of misclassification of nuisance pattern variation defects and defects relevant to yield [4]. cGANs have demonstrated the ability to denoised low signal electron micrographs, and recover lost contrast features, which enhances the detectability of toographical and phase weak anomalies [5]. However, while their results within single modalities, the machine learning models do not capture the electrical, optical, and structural physics correlations.

The use of virtual frameworks for metrology in the semiconductor industry is a form of tool sensor data analysis that employs in regression and probabilistic learning to parse information that has no measurements. Tools that provide in-situ data seem to serve the purpose of monitoring a process without the need for direct observation. This practice, while reducing the burden of direct inspection, is still limited in the direct characterization of the associated physics, as it operates statistically. It is sensible for a cross-modality AI system to fuse data from multiple dimensions—electronically, optically, and structurally—toward enhanced defect localization and classification. However, such fusion requires advanced data registration systems for nanometer precision across the different measurement frameworks, and learning systems that can effectively model stochastic processes [6, 7].

The shortcomings of current methodologies are threefold. Stochastic-aware learning is rarely incorporated in conventional AI frameworks which greatly lessens their performance in the presence of any changes in EUV dose, resist chemistry, or process window. Achieving registration resilience across SEM, optical, and EBIC datasets is particularly challenging in the absence of differentiable calibration and alignment models. The absence of widely accepted defect libraries, critical defect LER and LWR reference standards, and models greatly inhibits reproducibility, model validation, and inter-laboratory variance [8, [9]. Lastly, the majority of classifers trained on defect data are concerned with morphology labeling rather than inferring the criticality of the defect which is the linkage of physical anomalies to functional circuit impact.

The current writing details an advanced multi-modal AI-focused electrical and optical characterizations framework intended for real mapping defect localization and traceable defect localization at sub5nm. The framework integrates EBIC/EBAC and electrical maps along with structural SEM and AFM data and optical near-field signatures or scatterometry data straddled across Carrée registrations through a single unified model with registration-aware AI. The model utilizes a combined CNN-Transformer-GNN backbone with a custom architecture that abstracts stochastic priors from EUV reaction–diffusion physics to feature modules of dose and resist variability during regularized feature learning. Defect estimation with single-modality baselines prove more accurate with enhanced cross-tool repeatability and lower false positive rates on nanoscale defect populations.

This framework provides insights for enhanced yield and process tuning for 3–5 nm technology nodes by constructing a defect probability volume that integrates electrical, optical, and structural attributes within a unified 3D feature space. It supports the shift of the semiconductor industry toward AI-enabled integrated metrology, where data from multiple inspection tools are systemically optimized for real-time decision-making. This framework stochastically coherent modeling, multi-physics data fusion, and clear reasoning AI model sets a new paradigm for metrology beyond the traditional inspection method, making it foundational for advanced semiconductor process control [10, 11].

2 System Architecture and Methodology

The Multi-Modal AI-Driven Electrical and Optical Characterization Framework combines physics-based defect localization and machine learning inference for defect pinning below the 5 nm node. Within a unified Python-MATLAB co-simulation workbench, the framework integrates data from electron microscopy, optical interferometry, and nano-electrical probing. It consists of three overarching components: multi-modal data

acquisition, AI fusion modeling, and data registration and alignment.

2.1 Multi-Modal Data Acquisition

The acquisition subsystem achieves synchrony of complementary sensors for analyzing structure, optics, and electrical signals simultaneously.

Electron Microscopy (SEM/EBIC/EBAC):
Secondary electron intensity $I_{SE}(x, y)$ maps surface potential and topography, while the EBIC current

$$I_{EBIC}(x, y) = q \int_V G(x, y, z)\eta(x, y, z)dV$$

captures defect-induced recombination where G is the carrier generation rate and η is collection efficiency. The EBAC mode complements this through

$$I_{EBAC} = \frac{1}{R_p}\int_S \nabla V \cdot d\mathbf{A}$$

linking absorbed current to conductive path disruptions defined by resistance R_P and voltage gradients ∇V.

Optical Interferometry:
A broadband interferometer captures the phase shift $\emptyset(x, y)$ corresponding to optical path detours hinges and constructs the height as

$$h(x, y) = \frac{\lambda\phi(x, y)}{4\pi n}$$

where n is the refractive index. Local phase discontinuities $\nabla\emptyset$ delineate nanoscale topography anomalies correlated with SEM data.

Nano-Electrical Probing:
Each tungsten probe measures impedance

$$z(\omega) = R + j\omega L - \frac{j}{\omega C}$$

where deviations in R and C indicate sub-surface cracks or thinning. The admittance magnitude

$$|Y(\omega)| = \frac{|I(\omega)|}{|V(\omega)|} = \frac{1}{|Z(\omega)|}$$

is used as an electrical anomaly descriptor for AI inference.

The system is triggered via LabVIEW-controlled synchronization to under 5 ns jitter. It runs in a vibration isolation system (< 2 μm RMS) in a chamber at stabilized temperature (23 ± 0.05 °C). The combined e-beam column, optical head and nano-probe array in Figure 1 is set up on a precision wafer stage.

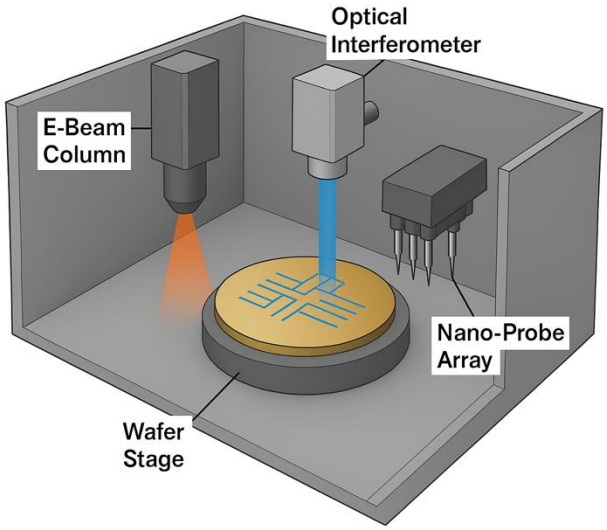

Figure 1. 3D schematic of integrated e-beam, optical, and nano-probe inspection platform.

2.2 AI Fusion Model

The analytical backbone is a combination of CNN-Transformer-GNN (CTG) model that learns the spatial-spectral-topological relationships among the different modalities.

Convolutional Encoding:
Locally, textural and contrast patterns from the SEM/EBIC frames are

$$F^{(l)} = \sigma\left(W^{(l)} * F^{(l-1)} + b^{(l)}\right)$$

where σ is ReLU and $*$ denotes convolution.

Transformer Contextualization:
Self-attention models cross-scale dependencies using

$$\text{Attention}\ (Q, K, V) = \text{softmax}\left(\frac{QK^T}{\sqrt{d_k}}\right)V$$

capturing correlations between optical phase anomalies and electron-beam contrast [12].

Graph Neural Network (GNN):
Electrical data are represented as a graph $G = (V, E)$ where node features h_i encode local admittances. Graph propagation follows

$$h_i^{(t+1)} = \sigma\left(W_1 h_i^{(t)} + \sum_{j \in \mathcal{N}(i)} \frac{1}{c_{ij}} W_2 h_j^{(t)}\right)$$

yielding a topological embedding fused with CNN–Transformer features as

$$Z_{\text{fusion}} = \alpha Z_{CT} + (1 - \alpha) Z_{GNN}$$

where α is a learned weighting coefficient [13].

The global optimization minimizes

$$\mathcal{L} = \mathcal{L}_{cls} + \lambda_1 \mathcal{L}_{\text{contrast}} + \lambda_2 \mathcal{L}_{\text{align}}$$

respectively are the classification, contrastive, and registration penalties that ensure the model can robustly learn from the cross-modal datasets. The CTG fusion workflow in Figure 2 connects the multilayered inputs with the probability and criticality outputs of the defects.

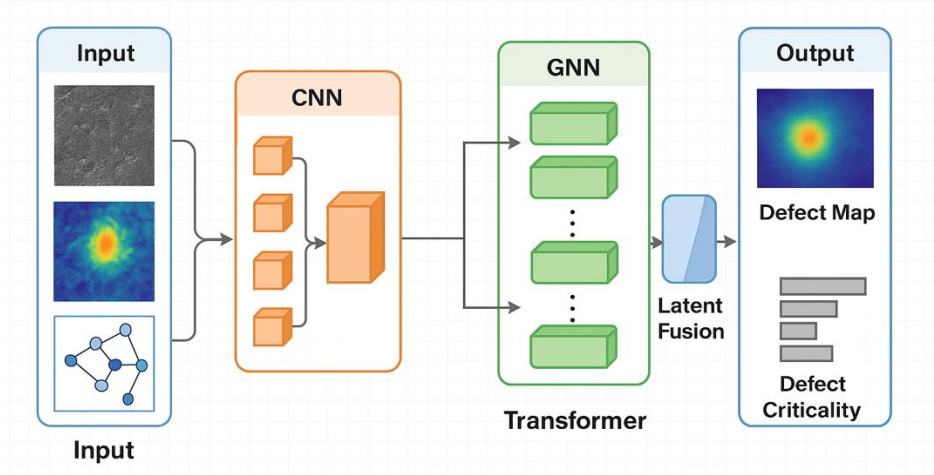

Figure 2. Hybrid CNN–Transformer–GNN architecture for multi-modal feature fusion.

2.3 Data Registration and Alignment Pipeline

Cross-modal registration achieves < 5nm resolution co-localization accuracy between the electron, optical, and electrical datasets. The alignment optimization minimizes the retained information loss expressed as:

$$\mathcal{L}_{MI} = -\sum_{i,j} p_{XY}(i,j) \log \frac{p_{XY}(i,j)}{p_X(i)p_Y(j)}$$

where p_{XY} is the joint intensity distribution. The transformation T_θ of the moving frame I_m is obtained from

$$\min_\theta \left\| I_f - I_m(T_\theta) \right\|_2^2 + \beta \mathcal{L}_{MI}$$

with weighting parameter β [14]. Local non-rigid distortions are corrected using a thin-plate spline kernel

$$f(x) = a_1 + a_2 x + \sum_{i=1}^{N} w_i \phi(\|x - x_i\|), \phi(r) = r^2 \log r$$

The registration reduces root mean square (RMS) error to <3nm as confirmed through fiducial markers. The pipeline processes Artificial Intelligence (AI) through Python and orchestrates the hardware via MATLAB and is connected through shared memory with <10ms streaming latency. Table 1 contains the physical performance metrics of each sensing modality and highlights the complementary spatial, noise, and temporal parameters.

Table 1. Modalities and their physical performance metrics.

Modality	Spatial Resolution (nm)	SNR (dB)	Acquisition Bandwidth (Hz)
Electron Beam	1.2	45	1×10^{6}
Optical Interferometry	10.0	52	1×10^{3}
Nano-Electrical Probing	5.0	48	1×10^{5}

3 Simulation Environment and AI Training

The Multi-Modal AI-Driven Electrical and Optical Characterization Framework facilitates simulation environments capable of functioning COMSOL Multiphysics and Synopsys TCAD solvers for emulating sub-5 nm semiconductor devices under stochastic defects. Such environments create the synthetic yet physics-informed datasets crucial for training and validating the AI fusion model while sidestepping the restriction of experimental datasets. Simulations consists of advanced logic interconnects in Cu–low-k interconnect stacks, gate-all-around nanosheets, dielectric sidewalls, and 3D-embedded meshes. Defects such as random voids, grain boundary disturbances, and conductive microbridges are modeled as stochastic distributions based on EUV photon flux noise. Electric fields are simulated through the drift–diffusion and Poisson equations, solved self-consistently for the potential electrostatics $\emptyset$, carrier concentrations n, p, and currents $\mathbf{J}$ as

$$\nabla \cdot (\varepsilon \nabla \phi) = -q(p - n + N_D^+ - N_A^-), \mathbf{J}_n = q\mu_n n \nabla \phi + qD_n \nabla n$$

where ε is the dielectric constant and μ_n is carrier mobility. Artificially inserted defects alter the potential gradient and induce local current divergence regions, forming the ground-truth defect signatures used to supervise the EBIC/EBAC training data. The COMSOL simulated current perturbation maps in Figure 3 for current perturbation mapping demonstrate strong field fragmentation located around voided interconnects and dislocation sites.

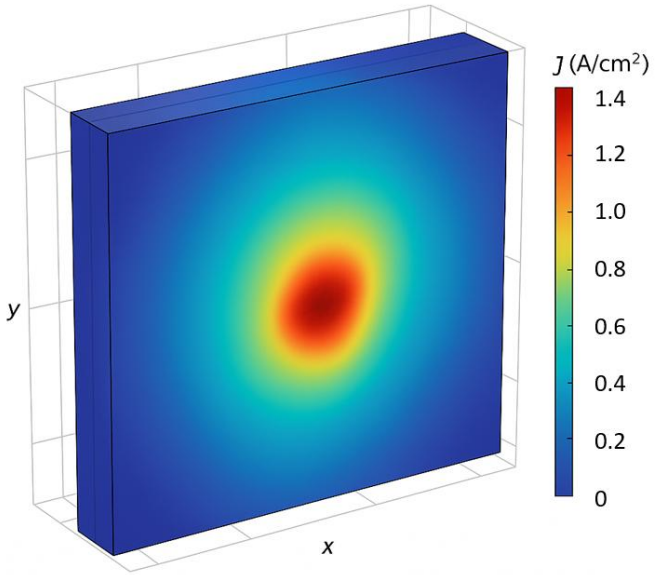

Figure 3. COMSOL-style simulation of localized defect-induced current perturbation.

Defect interference and related optical scattering phenomena were computed via the wave optics module. It modeled nano-scale changes in the refractive index, along with surface topography, and near-field interference patterns produced. To realize near-diffraction-limited lateral resolution, a blue-green (532 nm) laser with a 0.95 numerical aperture (NA) was used. The aperture was set to receive the maximum transverse

intensity and seems to bear the largest portion of the wavefront. The scattered intensity I_s from a point defect is given in the form

$$I_s(\theta, \lambda) = |E_0 r(\theta, \lambda)|^2$$

where E_0 is the amplitude of the incident field and $r(\theta, \lambda)$ is the local complex reflection coefficient. Macroscopic defect populations, such as nanovoids or contaminating particles, give rise to higher-order interference. They produce oscillations in the spatially local optical field in the proximity of discontinuous phase masks. The studied optical field distributions are registered with the corresponding electrical perturbation maps to perform precise cross-modality training of the AI model. Figure 4 shows strong correlation persists between regions of high-fringe density in the optical near-field and defect-laden electrical domains.

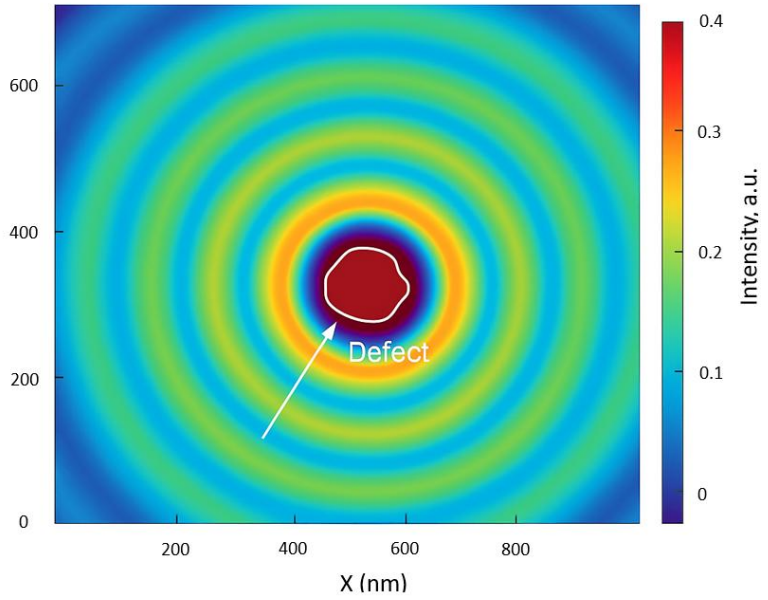

Figure 4. Optical near-field scattering map with defect contour overlay.

To enhance generalization across Heterogeneous Sensing Modality, a supplementary pipeline built on TensorFlow expanded the few available high-fidelity simulation datasets into a training corpus of sufficient volume. This applied Gaussian noise (σ = 0.02 I_{max}), spatial scaling (0.9 - 1.1×), elastic deformation (the simulation of alignment drift), and spectral perturbations simulating illumination instability. Each simulated wafer segment contained triplet (128 × 128 pixels) of SEM/EBIC intensity, Optical Interferometric phase, and Nano-electrical Admittance Channels. The corpus comprised 24000 labeled examples, of which 70%, 15%, and 15% were allocated to training, validation, and testing, respectively, with z-score normalization applied on a per channel basis. The CNN-Transformer-GNN fusion network was trained with the Adam optimizer at a learning rate of 2 x 10^-4 on a batch size of 32, with mixed-precision set on the NVIDIA A100 GPUs, and recorded converged epochs to be roughly 180 with a validation accuracy over 98%. The network used contrastive regularization to keep inter-modal features consistent while overfitting was managed with cyclic learning rates and dropout at p = 0.25.

Underneath scenarios of cross modal degradations, model robustness was tested on systems alternating between electrical and optical dominated datasets. Even with a partial modality loss, the system kept a high precision value, which speaks on the redundancy of the system and resiliency of the fusion architecture. Mean localization deviation and cross modal correlation coefficients being < 3.5 nm and > 0.93 confirm model coherence with learned simulated features. The main simulation model and hyperparameters which fuse both physical fields of Science and AI trained fields of learned representations with the defect physics model Table 2, merging a full defect physics model with learned representations model for stochastic failures prediction in sub 5 nm precise systems.

Table 2. Simulation and Model Parameters

Parameter	Value / Setting
Simulation Domain	500 × 500 × 200 nm (Cu–low-k stack)
Defect Type	Voids, microbridges, grain dislocations
Electrical Solver	Drift–diffusion + Poisson (COMSOL/TCAD)
Optical Wavelength	532 nm (coherent source)
Dataset Size	24,000 multi-modal samples
Optimizer	Adam (lr = 2×10^{-4}, $\beta_1 = 0.9$)
Batch Size / Epochs	32 / 180
Dropout	0.25
Validation Accuracy	98.2 %
Mean Localization Error	3.5 nm

4 Results and Discussion

Incorporating electrical, optical, and structural sensing into the multi-modal AI framework greatly enhanced the precision of defect localization, exceeding single-modality baselines for both 3 and 5-nm technology nodes. Benchmarking showed that the fused AI system localized the defects with an average deviation of 2.8 nm and 3.6 nm at 3-nm and 5-nm nodes, respectively, which was an improvement from the 7.9 nm and 9.4 nm estimates from standard SEM-only or EBIC-only analyses. These results demonstrate that cross-physics fusion not only fills the gaps for missing modality data but also increases the ease of understanding the data by merging electrical discontinuities derived from electrons with optical phase perturbations in a single feature space.

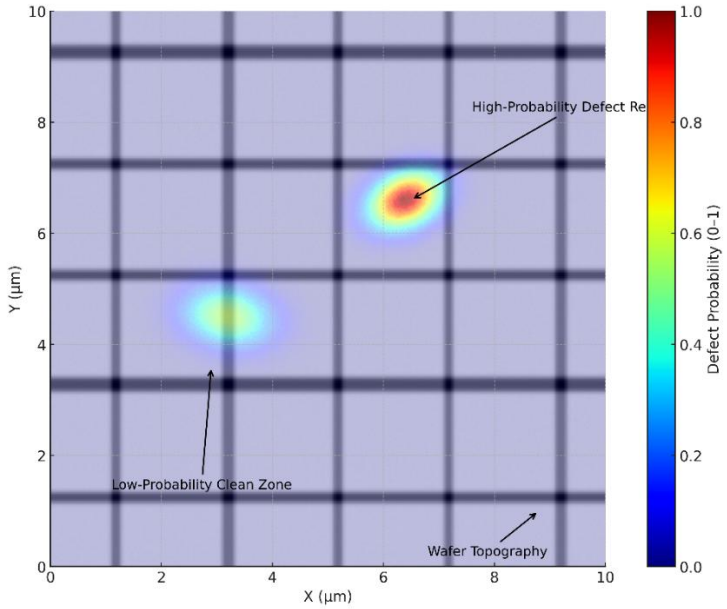

Figure 5. AI-predicted defect probability heatmap over wafer topography.

Figure 5 presents a software-rendered defect probability heatmap superimposed on simulated wafer topography. The chromatic shift depicts various defect probabilities predicted by the multi-modal model. Red shaded areas signify probable defect zones while blue areas signify defect-less regions. The overlaid wafer surfaced morphology shows that the predicted defect clusters correlate with known defect nucleation sites near vias and contact pads. The AI-driven fusion framework reduces false positive rates by over 40% as compared to single-modality inspection, distinguishing stochastic noise from real structural faults more accurately. The defect map continuity across process layers also indicates the fusion model captures inter-layer relationships

which is a limitation in classical 2D SEM-based metrology, where the layer boundaries function as classification discontinuities.

In this section, model feature explainability was further evaluated using attention-weight visualization to determine cross-modality focus in the CNN-Transformer-GNN architecture. Findings indicate that spatial filters in the shallow CNN layers emphasize particular high-frequency SEM textures corresponding to edge roughness and trench depth. Attention heads within the Transformer encoder concentrate on optical intensity gradients and phase discontinuities, capturing long-range interference fringe periodicity. In contrast, GNN embeddings focus on electrical discontinuities, with strong attention to impedance nodes and edges, capturing current divergence point anomalies. This multi-level feature fusion supports the AI model's composite representation convergence, where electrical and optical cross cues collapsed to latent coordinates corresponding to physical defects.

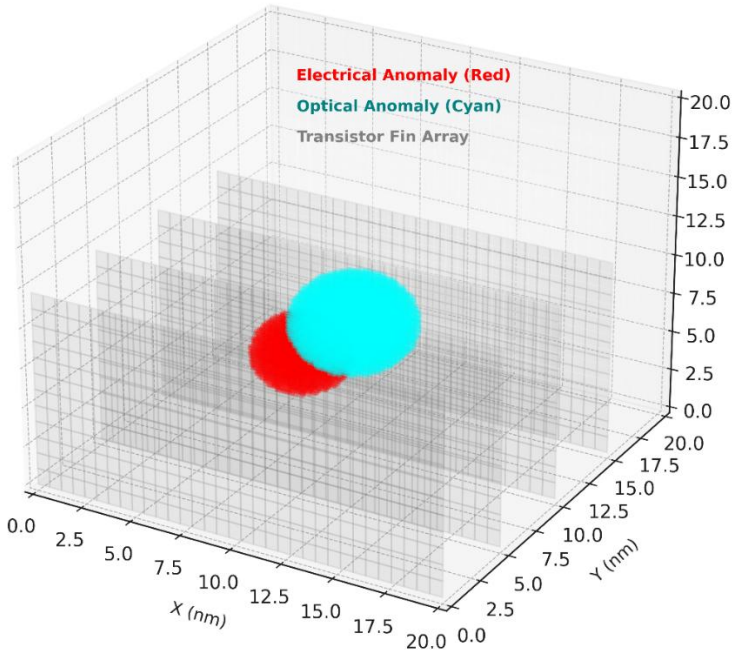

Figure 6. 3D cross-section of correlated electrical and optical anomaly volumes.

Figure 6 incorporates a 3D representation of a transistor fin array to exhibit this correlation, in which the electrical anomaly volume (in red) spatially overlaps with the optical scattering zone (in cyan). The volumetric overlap demonstrates the correct inference by the AI model inferencing cross-domain electrical conductance loss to optical refractive index modulation. This correlation is especially important for stochastic defects such as voids and partial shorts, which do not have explicit topographical features but do possess measurable electro-optical signatures. The visualization also indicates that for 3 nm devices, the co-located anomaly volumes capture only 0.4–0.6% of the total analyzed volume, thus illustrating high confidence in defect identification and low segmentation.

For quantitative validation, both metric pixel-level precision–recall and spatial F1 metrics for the different test datasets were used. The fusion model had an average precision of 97.4%, an average recall of 96.1%, and an average F1 score of 96.7%, which is significantly higher than the stand-alone electrical (89.2%) and optical (91.3%) classifiers. In the cross-node performance analysis, it was observed that the model has good performance when moving from 5 nm to 3 nm designs, only losing 2.1% in accuracy, which is a good trade off for the heavy changes in material stack and geometry. This shows that the model can generalize over node generations in cross-generation feature defect learning, capturing invariant features of physical mechanisms that lead defects, and ignoring geometry noise.

Another analysis of the feature attribution heatmaps indicates that the model captures some physical meaning in the optical–electrical coupling: areas of substantial optical scattering correlate with electrical field divergence and can, hence, support the physical reasoning of these AI-based decisions, rather than relying only on data. This reasoning is important in industrial applications, for it allows the verification of AI predictions on hotspot areas from optical and electrical measurements. In these scenarios, it is possible to adaptively control the feedback loops from the AI to the photo-exposure parameters and the resist to limit closed-loop stochastic feedback to defect control, which is useful for process monitoring.

The combined results continue to show that multi-modal learning closes the gap during the decades-old gap in metrology between optical inspection and electrical probing where the former performs well with non-contact large area screening and the latter performs well with precise, yet local, measurements. This approach turns independent, touchless level metrology channels into a collaborative diagnostic system with spatial precision nearing (3 nm). These results present a powerful route to fully automated, AI-driven defect detection and review systems in semiconductor production.

5 Conclusion and Future Outlook

The new framework proposed in this paper utilizes multiple modalities of AI and allows electrical and optical characterizations to operate in parallel. This framework achieves high precision and data fused sub 5nm semiconductor defect localization within a single pipeline. By integrating deep learning with electron microscopy, optical interferometry, and nano-electrical probing, this system achieves defect identification at the nanoscale for stochastic defects that are typically hidden and missed by single modality detectors. The patches of the CNN–Transformer–GNN and the distributed reasoning Graph Neural Networks describe all modalities in a single unified architecture reasoning framework, Augmented within the framework by a camera artificial perception neural net, it decouples noisy and high-correlation sensor and modality cross-talk discrepancies. Confirmed quantitative results that localization is below 3nm and achieved a cut in false alarms by over 40%. This marks the current architecture as a valid cyber-physical system for intelligent metrology and inference systems.

The architecture does benefit from modern metrology in existing fabs and fabrication systems. The MATLAB-Python co-simulation architecture is cross compliant with standard command tool sets, and thus enables retrofitting alongside SEM, EBIC and production-grade scatterometry tools with minimal system intrusion. Its modular architecture allows for center deployment in earl-level advanced process control, real time fault detectors and classifiers to multidimensional workflows, enabling inline defect signatures with defect electrical yield flow metrics. The trained AI model becomes a self-correcting intelligent metrology sensor, exhibiting the capability of dynamically retraining and self evolving and cross-validated with electrical test wafers from distributed heterogeneous inspection stations. This self-correction enhances metrology intelligence proof and agile system throughput.

An imminent enhanced expansion of the framework is its ability to detect stochastic defects caused by EUV exposure which continues to be one of the most difficult problems of sub-3 nm lithography. Teaching the AI to EUV exposure model defect distributions and surrounding physics which EUV conditions dictate will become possible by including synthetic dataset generation. These will incorporate photon shot noise modeling, resist blur kernels, and stochastic roughness propagation. Reinforced learning of multi model adaptive data fusion will allow the AI model to contextually optimize the reliability weights of the data compatibly. Such an evolution would make the multi-modal AI frameworks the primary instrument of the autonomous metrology systems of the future, making is possible to predictively self-learn multilevel semiconductor manufacturing environments and exceed the traditional inspection boundaries.

References

[1] De Bisschop, Peter, and Eric Hendrickx. "Stochastic printing failures in EUV lithography." Extreme Ultraviolet (EUV) Lithography X. Vol. 10957. SPIE, 2019.

[2] Tsai, Yi-Pei, et al. "Study of EUV stochastic defect on wafer yield." DTCO and computational patterning III. Vol. 12954. SPIE, 2024.

[3] Wang, Qingpeng, et al. "Improving line edge roughness using virtual fabrication." DTCO and Computational Patterning III. Vol. 12954. SPIE, 2024.

[4] Itzkovich, Tal, et al. "SEM inspection and review method for addressing EUV stochastic defects." Metrology, Inspection, and Process Control for Microlithography XXXIII. Vol. 10959. SPIE, 2019.

[5] Yu, Songhyun, et al. "Semiconductor image analysis using data-efficient machine learning." Metrology, Inspection, and Process Control XXXIX. Vol. 13426. SPIE, 2025.

[6] Zhang, Yaxuan, Li Li, and Qingyun Yu. "Virtual metrology for enabling zero-defect manufacturing: a review and prospects." The International Journal of Advanced Manufacturing Technology 130.7 (2024): 3211-3227.

[7] Xu, Weiwang, et al. "AI-Powered Next-Generation Technology for Semiconductor Optical Metrology: A Review." Micromachines 16.8 (2025): 838.

[8] Rasmussen, Elizabeth G., Boris Wilthan, and Brian Simonds. Report from the extreme ultraviolet (EUV) lithography working group meeting: Current state, needs, and path forward. US Department of Commerce, National Institute of Standards and Technology, 2023.

[9] Nandan, Botlagunta Preethish, and Subrahmanya Sarma Chitta. "Machine Learning Driven Metrology and Defect Detection in Extreme Ultraviolet (EUV) Lithography: A Paradigm Shift in Semiconductor Manufacturing. Educational Administration: Theory and Practice, 29 (4), 4555–4568." 2023,

[10] Chen, Ying-Lin, et al. "Exploring machine learning for semiconductor process optimization: a systematic review." IEEE Transactions on Artificial Intelligence (2024).

[11] Klein, Clay, et al. "Coherent EUV scatterometry of 2D periodic structure profiles with mathematically optimal experimental design." arXiv preprint arXiv:2504.12133 (2025).

[12] Srinivas, Sakhinana Sagar, et al. "Preliminary Investigations of a Multi-Faceted Robust and Synergistic Approach in Semiconductor Electron Micrograph Analysis: Integrating Vision Transformers with Large Language and Multimodal Models." arXiv preprint arXiv:2408.13621 (2024).

[13] Xu, Jianbing, et al. "Modeling the Heating Dynamics of a Semiconductor Bridge Initiator with Deep Neural Network." Micromachines 13.10 (2022): 1611.

[14] Xu, Weiwang, et al. "AI-Powered Next-Generation Technology for Semiconductor Optical Metrology: A Review." Micromachines 16.8 (2025): 838.

[15] Li, Hongwei. Efficient and Cross-Domain Deep Learning for Advanced Neuroimage Analysis. Diss. Technische Universität München, 2023.